Supporting Information

Dual peptide nanoparticles platform for enhanced antigen-specific immune tolerance for treatment of experimental autoimmune encephalomyelitis

Huangwei Wang,[a,b,§] Jun shang,[d,e,§] Zhesheng He,[a] Miaomiao Zheng,[a,b] Huiju Jia,[a,b] Yaning zhang,[d] Wenzhi Yang,*[b] Xueyun Gao[c] and Fuping Gao*[a]

[a] CAS Key Laboratory for the Biological Effects of Nanomaterials and Nanosafety, Institute of High Energy Physics, Chinese Academy of Sciences, Beijing 100049, China

[b] School of Pharmacy, Hebei University, Baoding 071002, China

[c] Department of chemistry and biology, Beijing University of Technology, Beijing 100124, China

[d] Linfen People's Hospital, Shanxi 041000, China

[e] Tianjing Medical University General Hospital, Tianjin 300052, China

[§] Contributed equally to this work

*Email : gaofp@ihep.ac.cn, yangwz@hbu.edu.cn

1. Supplementary Tables

Table S1. The influence of different ultrasound time and power on the size of nanoparticles

Ultrasound power (%)	Ultrasound Time (min)	Particle Size (nm)
20	2	431.83
19	2	481.70
18	2	556.58
16	3	394.47
15	3	501.44
15	4	386.70

Table S2. The influence of the concentration of emulsifier (PVA) on the size of nanoparticles

the concentration of PVA (m:V)	Particle Size (nm)
0.5%	391.57
1%	440.98
1.5%	472.07
2%	501.44
3%	565.74
4%	804.79

Table S3. The influence of the concentration of PLGA on the size of nanoparticles

Concentration of PLGA (mg/mL)	Particle Size (nm)
10	466.89
20	465.71
30	501.44
40	500.01
50	554.55

Table S4. The influence of water-oil two-phase volume ratio on the particle size of nanoparticles

Volume Ratio of W_2 and O (V/V)	Particle Size (nm)
10：1	291.25
15：1	329.03
25：1	501.44
35：1	590.69
45：1	1217.41

Table S5. The effect of the concentration of PLGA on peptide loading of nanoparticles

Concentration of PLGA (mg/mL)	Peptide Loading (μg/mg)
10	1.32
20	1.46
30	2.17
40	2.54
50	3.26

Table S6. The influence of the concentration of LABL on the peptide loading of nanoparticles

Concentration of LABL (mg/mL)	Peptide Loading (μg/mg)
10	1.02
15	1.53
20	2.17
25	2.54
50	3.74

Table S7. The influence of the concentration of MOG_{35-55}-KKK on the peptide loading of nanoparticles

Concentration of MOG_{35-55}-KKK (mg/mL)	Peptide Loading (μg/mg)
5	4.67
10	7.43
15	11.24
20	16.79
25	17.21

2. **Supplementary Figures**

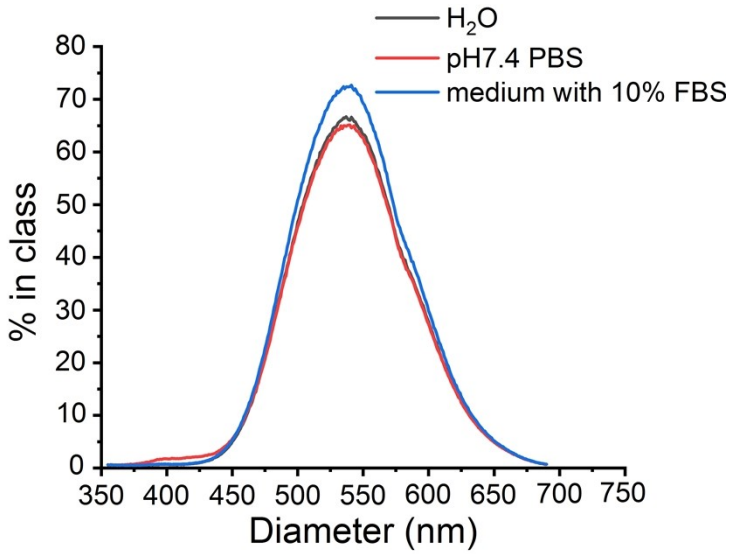

Figure S1. The average particle sizes of the dual peptide nanoparticles ($NPs_{LABL+MOG}$) when being dispersed in deionized water, pH7.4 PBS and medium containing 10% FBS.

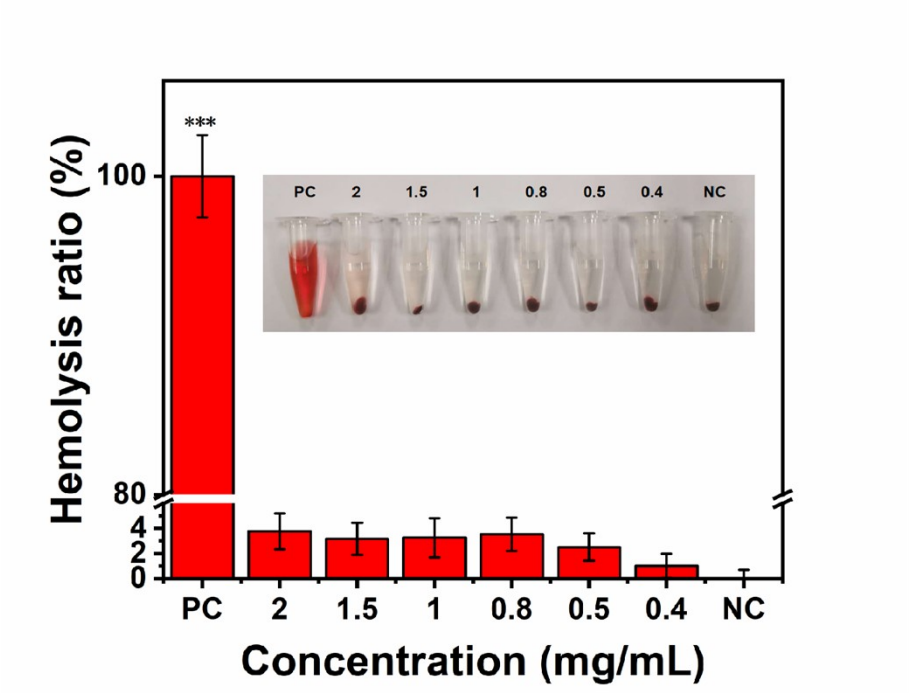

Figure S2. Relative hemolysis after incubation with different concentration of NPs $_{LABL+MOG}$ for 4 h, H_2O and PBS was used as positive control (PC) and negative control (NC), reapectively. ***P < 0.001 compared with NPs $_{LABL+MOG}$ group and PBS group, analyzed by student's t-test.

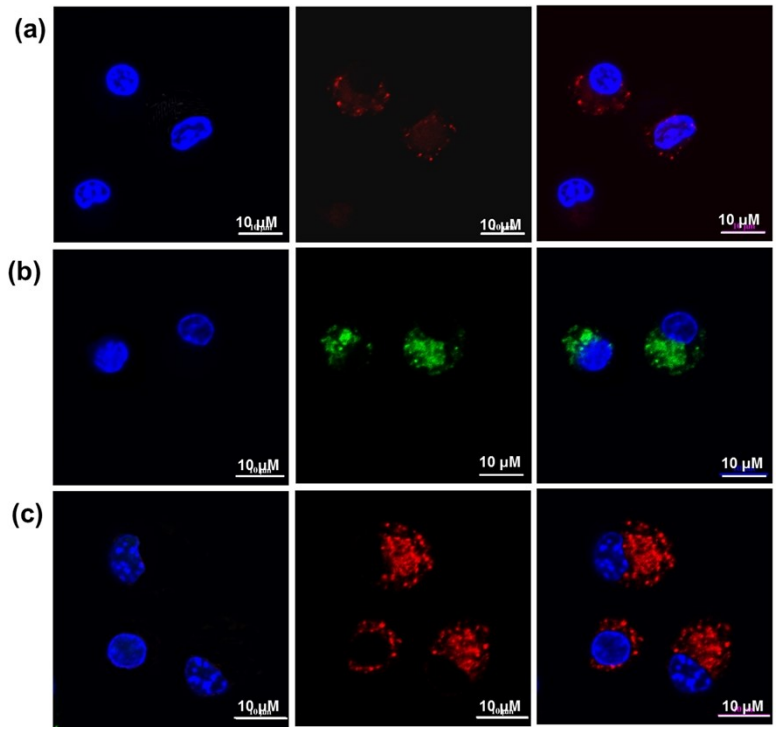

Figure S3. Confocal microscopy imaging of peptide nanoparticles uptake by DC2.4. (a) Cy5.5 labeled LABL NPs; (b) FITC labeled MOG_{35-55}-KKK NPs; (c) MOG_{35-55}-KKK and Cy5.5 labeled LABL NPs. The nuclei are stained with Hoechst 33342 which shows as blue fluorescence.

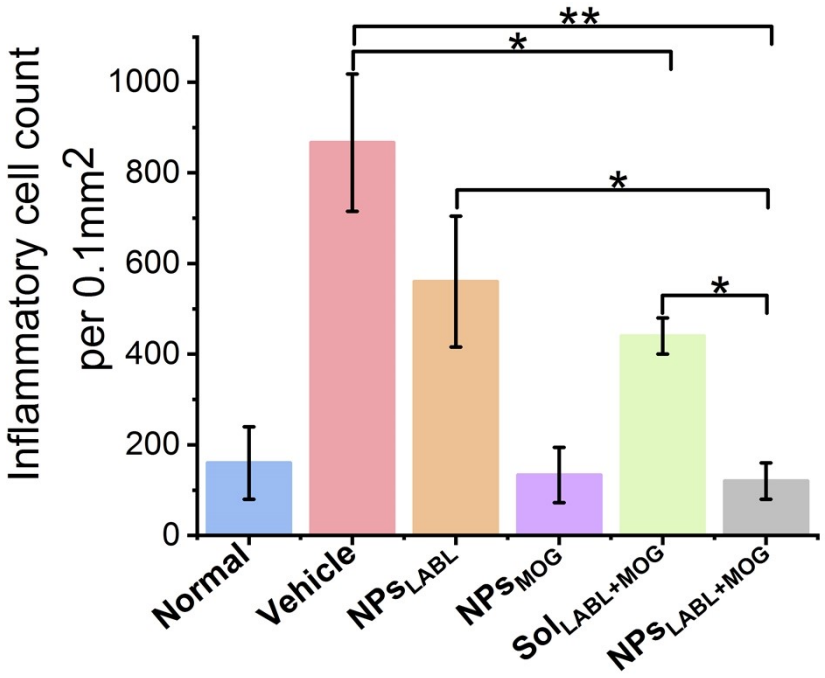

Figure S4. Average number of infiltrating inflammatory cells per unit area of spinal cord tissue in different treatment groups in the prophylactic experiment. The data were the average of hematoxylin and eosin (H&E) staining of three spinal cord tissues. *P <0.05, **P <0.01.

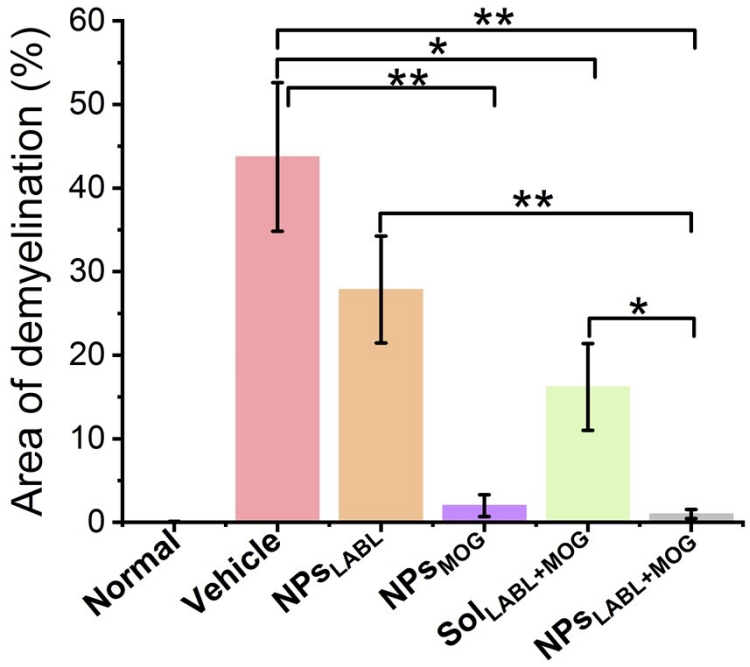

Figure S5. Percentage of damaged area of spinal cord tissue from different treated groups by luxol fast blue (LFB) staining in the prophylactic experiment. The data were the average of LFB staining of three spinal cord tissues. **P* <0.05, ***P* <0.01.

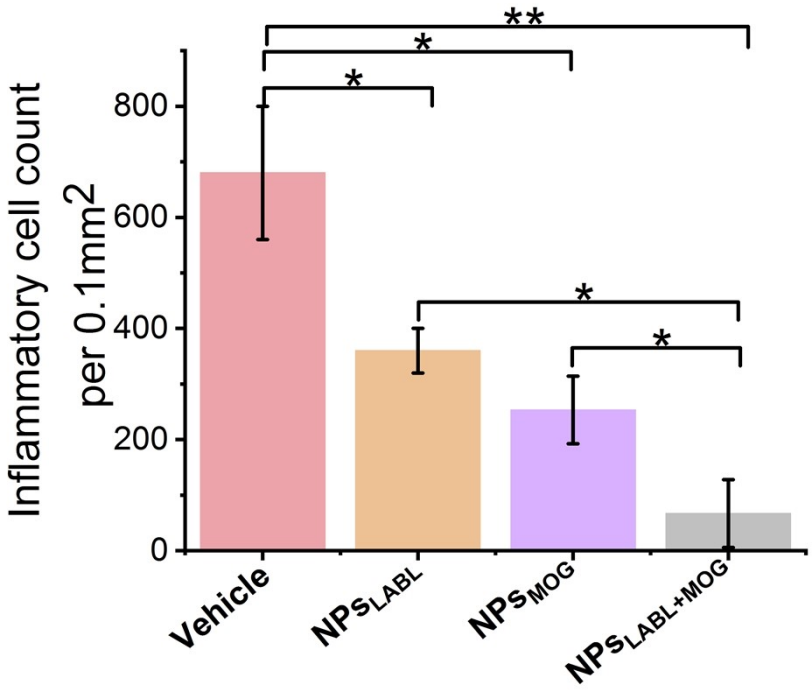

Figure S6. Average number of infiltrating inflammatory cells per unit area of spinal cord

tissue in different treatment groups in the treatment experiment. The data were the average of hematoxylin and eosin (H&E) staining of three spinal cord tissues. *P <0.05, **P <0.01.

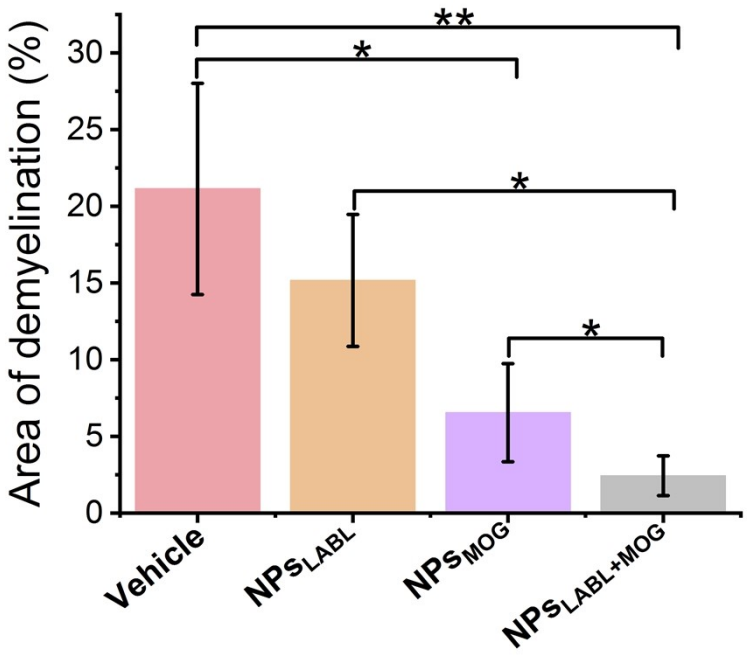

Figure S7. Percentage of damaged area of spinal cord tissue from different treated groups by luxol fast blue (LFB) staining in the treatment experiment. The data were the average of LFB staining of three spinal cord tissues. *P <0.05, **P <0.01.

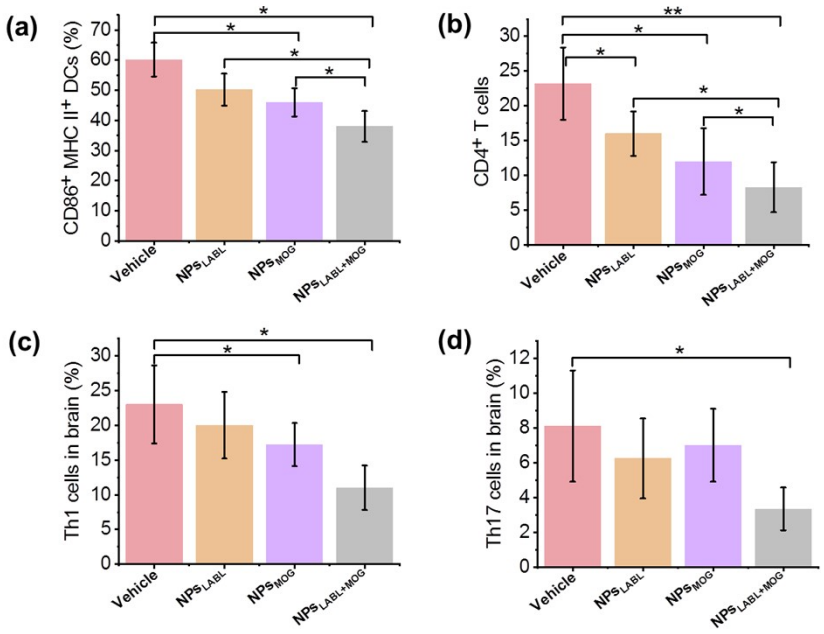

Figure S8. Average percentage of $CD86^+$ MHC II^+ DCs (a) and $CD4^+$ T cells (b) in splenocytes or Th1 cells (c) and Th17 cells (d) in brain. Date are the average of three independent experiments. *$p < 0.05$; **$p < 0.01$.

3. Supplementary Methods

Dendritic cells (DCs) culture and DCs uptake of peptide nanoparticles

A murine bone marrow derived dendritic cell line, DC2.4 were cultured in RPMI 1640 (Gibco) medium supplemented with 10% fetal bovine serum (FBS, Gibco), 100 μg/mL streptomycin, 100 IU/mL penicillin, 2 mM L-glutamine, 55 μM 2-mercaptoethanol (Gibco), 1× nonessential amino acids (Cellgro), and 10 mM HEPES (Invitrogen). The medium was exchanged every 2 days.

The uptake of peptide nanoparticles by DC2.4 was analyzed by laser confocal microscopy (CLSM). Immature DCs (1×10^6 cells per well) were seeded in 35 mm^2 glass bottom dishes for 24 h. The cells were then treated with fluorochrome labeled

peptide-loaded nanoparticles (NPs $_{LABL}$, NPs $_{MOG}$ and NPs $_{LABL+MOG}$) at the same concentration of LABL or MOG peptide for 4 h at 37 °C. The cells were washed with PBS and the nucleus were stained using 10 μg/mL Hochst 33342 in dark. After rinsing with PBS, the uptake of peptide-loaded nanoparticles by DC2.4 was imaged using CLSM (Nikon Ti-e microscope, Japan).